Towards high resolution Bayesian snow reconstruction in permafrost regions

K. Aalstad (Uni. Oslo; kristoffer.aalstad@geo.uio.no), S. Westermann (Uni. Oslo), L. Bertino (NERSC), T.V. Schuler (Uni. Oslo), J. Boike (AWI), J. Fiddes (SLF), L. Karsten (NCAR)

CESM LMWG, Boulder, 6th of Februrary 2018

SatPerm (NRC): Satellite-based Permafrost Modeling across a Range of Scales

- Aim: Constrain uncertainty in permafrost modeling induced by surface boundary conditions across a range of spatial scales and landscapes.
- Method: Offline assimilation of satellite retrievals into simple land surface schemes using ensemble-based data assimilation (DA).
- Validation: Multiple independent ground based observations.

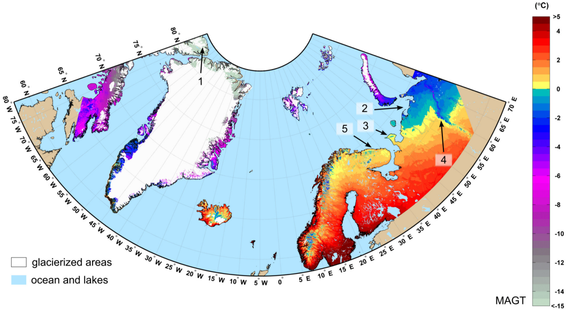

Figure : Satellite-based model estimates of MAGT from Westermann et al. (2015).

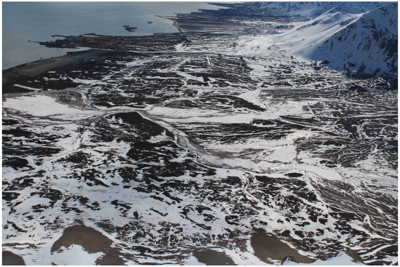

Figure : View over Bayelva and Ny Ålesund (Svalbard) taken by an automatic camera system under melting conditions on the 5th of June 2016.

Snow cover:

1. High albedo.
2. Low thermal conductivity.
3. Large water holding capacity.
4. Typically seasonal.
5. Rarely uniformly distributed.

$\Sigma =$ strongly modulates the surface energy and water balance.
$\longrightarrow$ distribution is a key control on permafrost.

Reconstructing the snow water equivalent (SWE) distribution through modeling alone is difficult, but what can we observe through existing earth observations?

Shorwave reflectances

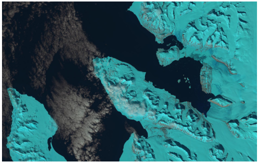

Figure : LandSat8 NC image ©NASA/USGS.
Resolution Direct Accurate Precise Gaps

PM SWE

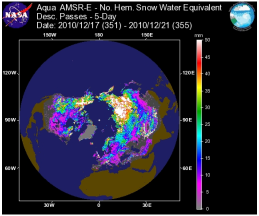

Figure : AMSR-E SWE composite ©NSIDC.
Resolution Direct Accurate Precise Gaps

Gravimetric TWS

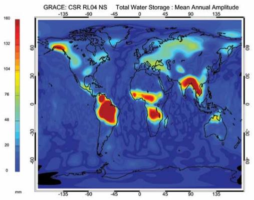

Figure : GRACE TWS composite ©NASA-JPL.
Resolution Direct Accurate Precise Gaps

Uncertanties in models (from parametrizations, discretization ...) and observations (from drift, noise ...) are due to generally *unknown* errors.

1. **Systematic error (bias, ME):** A mean departure from the true value, the inverse of accuracy.
2. **Random error (noise, RMSE):** A random (zero average) departure from the true value, the inverse of precision.
3. **Representativeness error:** Discrepancies in the scale of the model/observations and how these are interpreted.

By acknowledging that both models and observations are uncertain it is natural to cast these in a stochastic, as opposed to deterministic, framework.

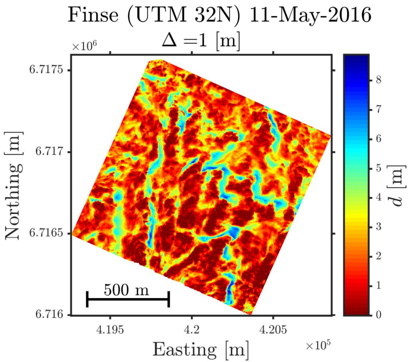

Figure : High resolution snow depth field retrieved from a drone (courtesy K. Gisnås NGI).

Data assimilation (DA) attempts to objectively fuse uncertain information from observations and models to provide an estimate of the state and parameter space of a dynamical system.

Approximate solution to the Bayesian estimation problem

$$\underbrace{p(\mathbf{x}|\mathbf{y})}_{\text{Posterior}} \propto \overbrace{p(\mathbf{y}|\mathbf{x})}^{\text{Likelihood}} \underbrace{p(\mathbf{x})}_{\text{Prior}}, \qquad (1)$$

i.e. **we seek the posterior: the probability of model trajectories *given* the observations.**

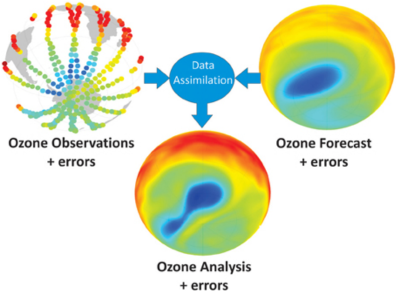

Figure : Adapted from Lahoz and Schneider (2014).

This talk will present:

1. A brief description of a Bayesian DA framework for snow reconstruction.
2. A case study carried out near Ny-Ålesund, Svalbard for several snow seasons.
3. An application of the framework to a mountain range in Japan for the 2016 snow season.
4. Initial results for two snow seasons in the Izas catchment in the Spanish Pyrenees.

Bayesian snow reconstruction (Durand et al., 2008): tries to represent the uncertainties in classical snow reconstruction (Slater et al., 2013).

- Model: Simple single-layer snowmelt (SEB/DD) models coupled to a probabilistic snow depletion curve (Liston, 2004).
- Obs: Satellite retrievals of fractional snow covered area (fSCA).
- Assimilation: Ensemble smoother with multiple data assimilation (ES-MDA; Emerick and Reynolds 2013).
- Forcing: Downscaling reanalysis data using TopoSCALE (Fiddes and Gruber, 2014) and a "LT" model (Schuler et al., 2008).

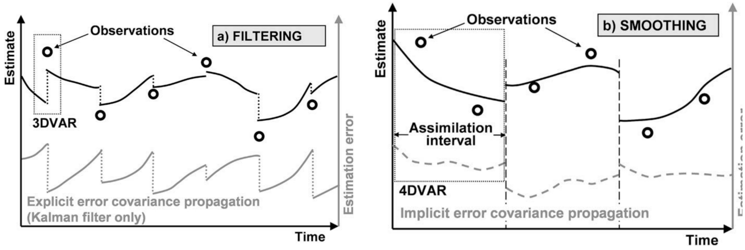

Figure : Adapted from Reichle (2008).

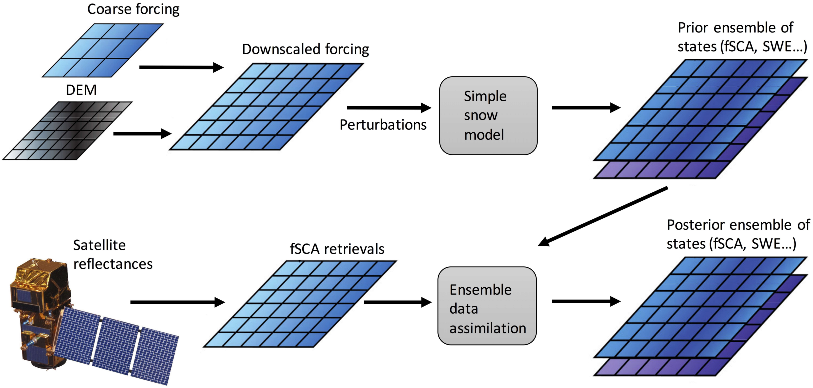

Figure : Simplified flowchart showing the work flow in the data assimilation framework, adapted from Durand et al. (2008).

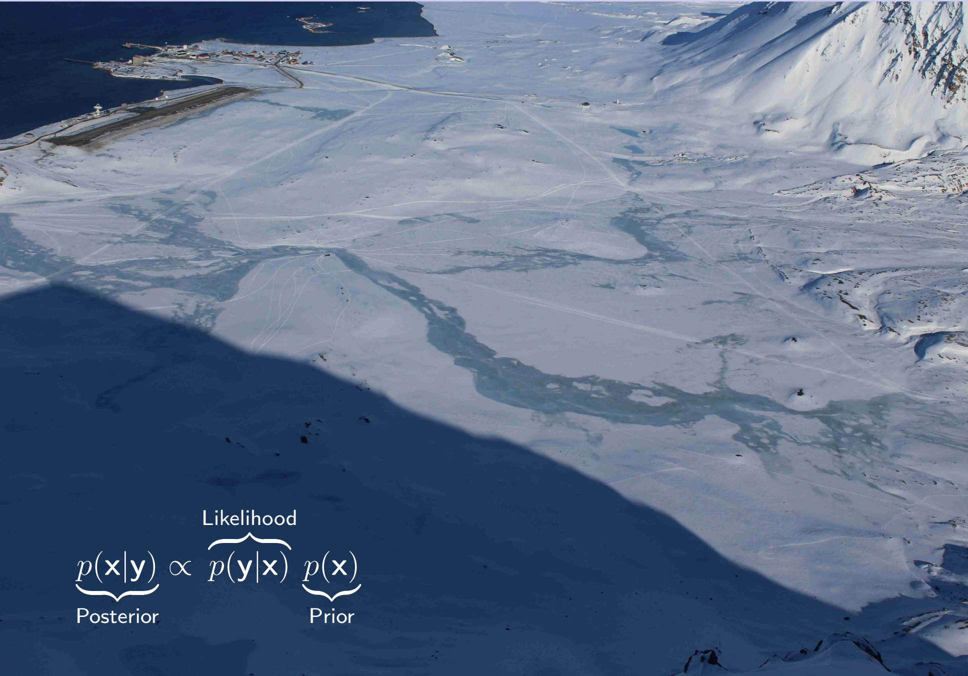

$$\underbrace{p(\mathbf{x}|\mathbf{y})}_{\text{Posterior}} \propto \overbrace{p(\mathbf{y}|\mathbf{x})}^{\text{Likelihood}} \underbrace{p(\mathbf{x})}_{\text{Prior}}$$

$$\underbrace{p(\mathbf{x}|\mathbf{y})}_{\text{Posterior}} \propto \overbrace{p(\mathbf{y}|\mathbf{x})}^{\text{Likelihood}} \underbrace{p(\mathbf{x})}_{\text{Prior}}$$

$$\underbrace{p(\mathbf{x}|\mathbf{y})}_{\text{Posterior}} \propto \overbrace{p(\mathbf{y}|\mathbf{x})}^{\text{Likelihood}} \underbrace{p(\mathbf{x})}_{\text{Prior}}$$

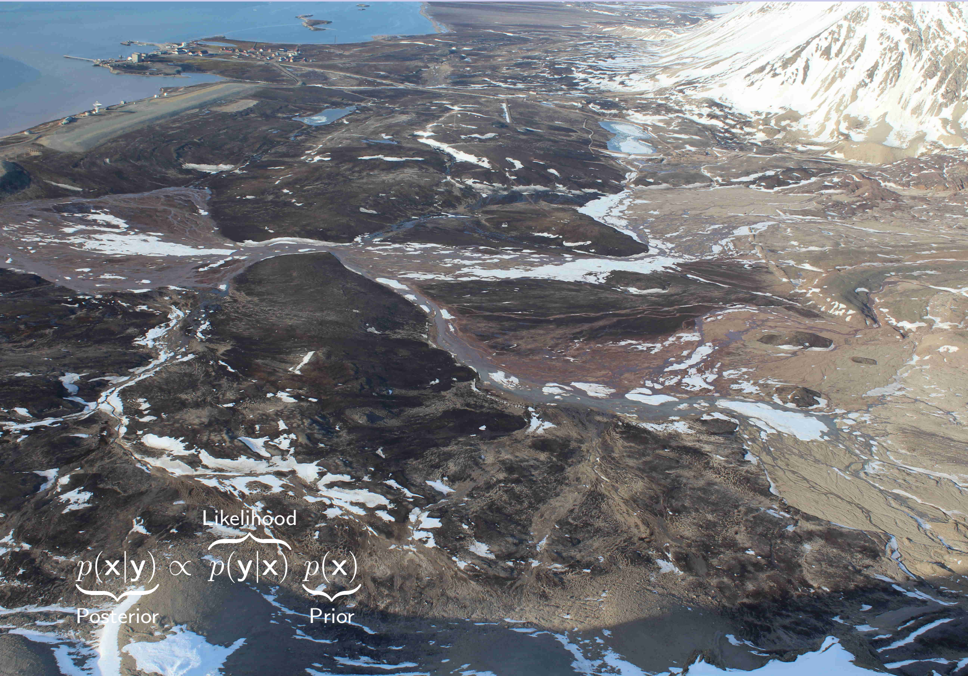
$$\underbrace{p(\mathbf{x}|\mathbf{y})}_{\text{Posterior}} \propto \overbrace{p(\mathbf{y}|\mathbf{x})}^{\text{Likelihood}}\ \underbrace{p(\mathbf{x})}_{\text{Prior}}$$

$$\underbrace{p(\mathbf{x}|\mathbf{y})}_{\text{Posterior}} \propto \overbrace{p(\mathbf{y}|\mathbf{x})}^{\text{Likelihood}} \underbrace{p(\mathbf{x})}_{\text{Prior}}$$

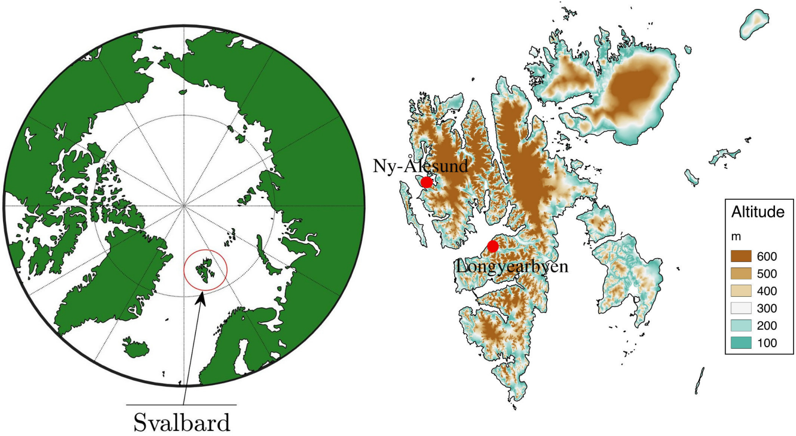

Figure : Location of the study area.

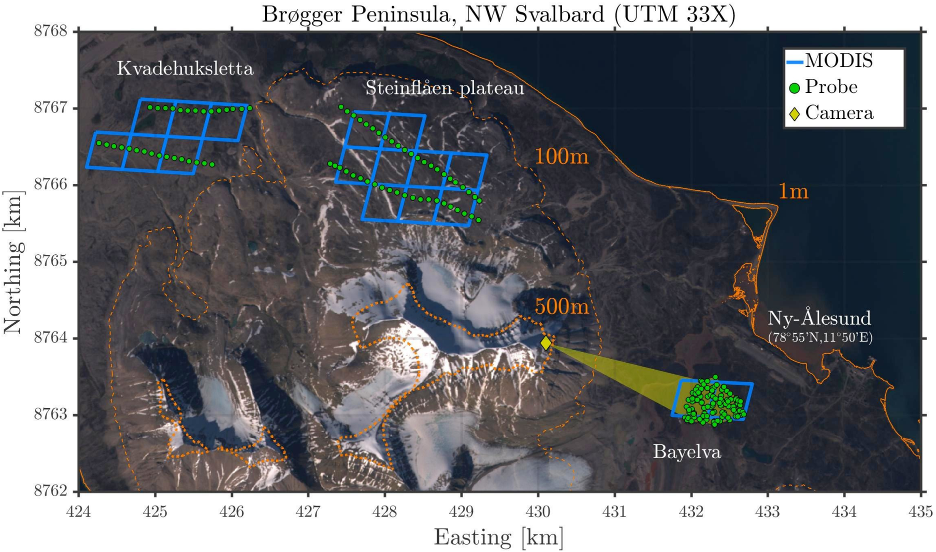

Figure : Domain superimposed on Sentinel-2A imagery taken 02.07.2016 (contours courtesy of NPI).

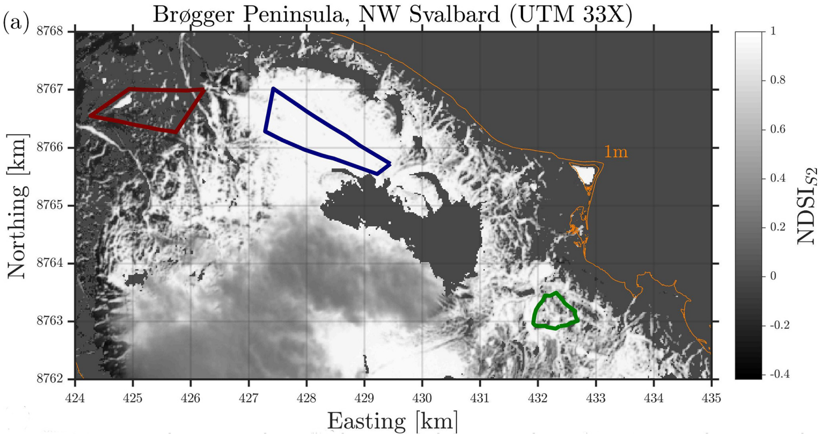

Figure : Sentinel-2 NDSI field (04.06.2016).

$$\mathrm{NDSI} = \frac{r_{\mathrm{VIS}} - r_{\mathrm{SWIR}}}{r_{\mathrm{VIS}} + r_{\mathrm{SWIR}}} \tag{2}$$

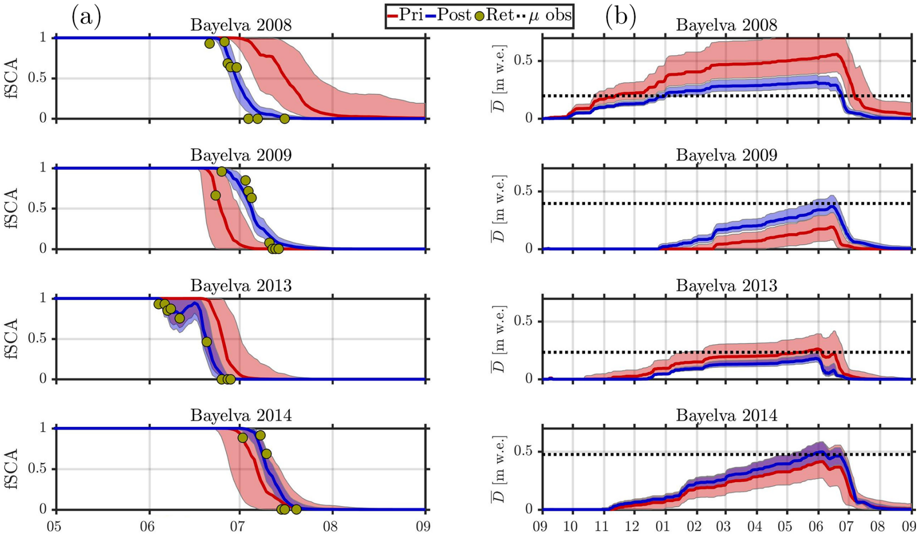

Figure : Prior (red) and posterior (blue) estimates of the fSCA (a) and mean SWE depth (b). Yellow dots show the fSCA retrievals while the dashed black lines show the independently observed peak mean SWE.

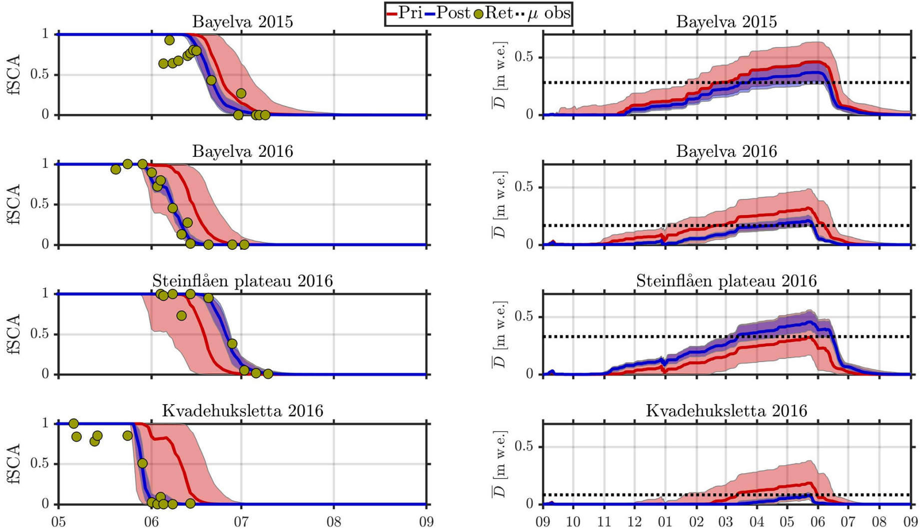

Figure : Prior (red) and posterior (blue) estimates of the fSCA (a) and mean SWE depth (b). Yellow dots show the fSCA retrievals while the dashed black lines show the independently observed peak mean SWE.

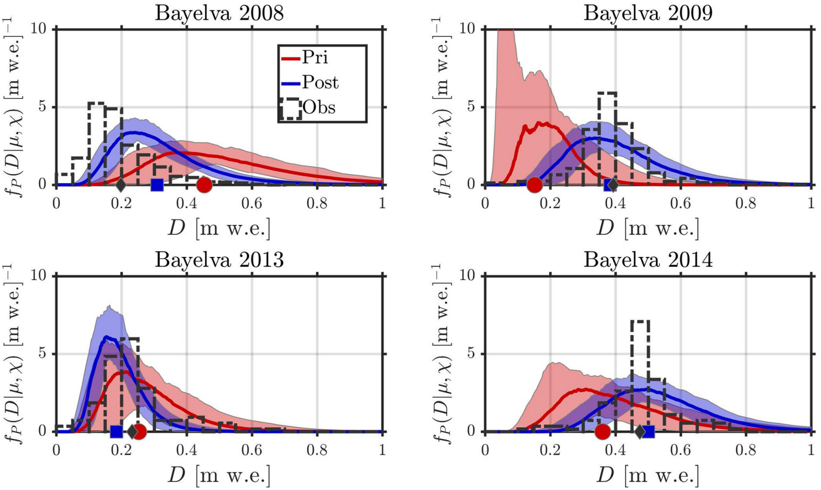

Figure : The posterior (blue) and prior (red) estimates of the subgrid snow distribution along with the corresponding observed distribution (dashed black). Markers show the mean of the respective distributions

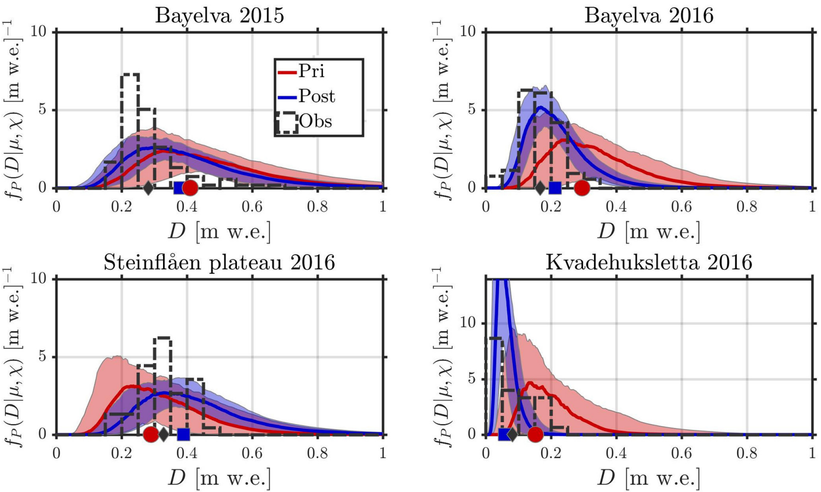

Figure : The posterior (blue) and prior (red) estimates of the subgrid snow distribution along with the corresponding observed distribution (dashed black). Markers show the mean of the respective distributions

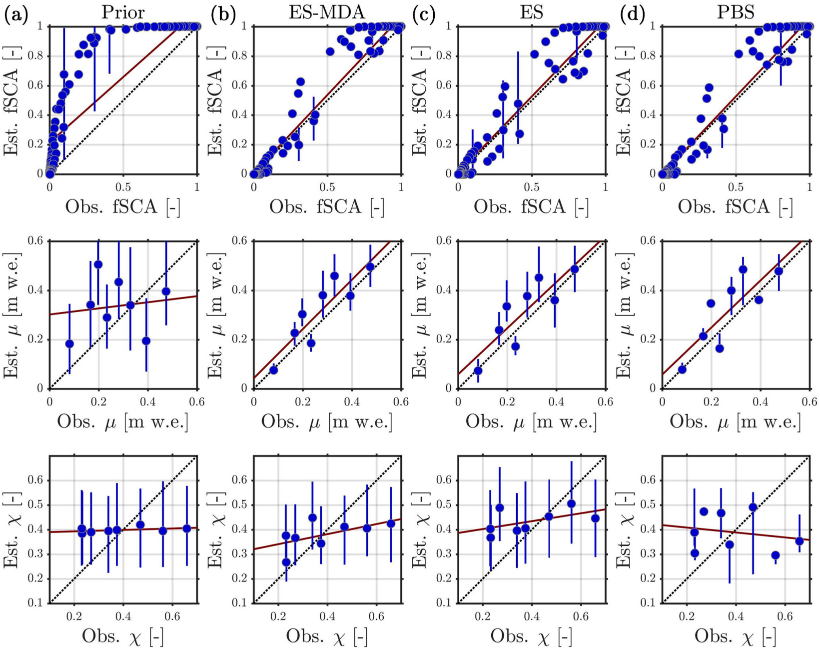
(a) Prior
(b) ES-MDA
(c) ES
(d) PBS
Est. fSCA [-]
Obs. fSCA [-]
Est. μ [m w.e.]
Obs. μ [m w.e.]
Est. χ [-]
Obs. χ [-]

The Cryosphere, 12, 247–270, 2018
https://doi.org/10.5194/tc-12-247-2018

The Cryosphere
Open Access
EGU

Ensemble-based assimilation of fractional snow-covered area satellite retrievals to estimate the snow distribution at Arctic sites

Kristoffer Aalstad[1], Sebastian Westermann[1], Thomas Vikhamar Schuler[1], Julia Boike[2], and Laurent Bertino[3]

[1]Department of Geosciences, University of Oslo, P.O. Box 1047, Blindern, 0316 Oslo, Norway
[2]Alfred Wegener Institute Helmholtz Center for Polar and Marine Research, Telegrafenberg A43, 14473 Potsdam, Germany
[3]Nansen Environmental and Remote Sensing Center, Thormøhlens gate 47, Bergen 5006, Norway

Correspondence: Kristoffer Aalstad (kristoffer.aalstad@geo.uio.no)

Received: 13 June 2017 – Discussion started: 4 July 2017
Revised: 1 December 2017 – Accepted: 12 December 2017 – Published: 23 January 2018

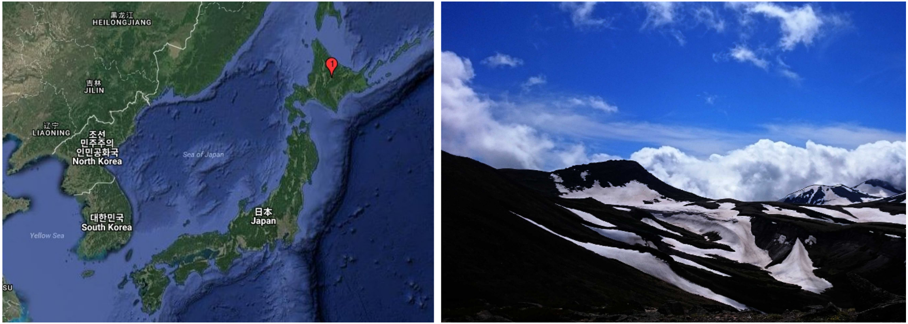

Figure : Left panel: Location of the Daisetsu mountains (Hokkaido, Japan) marked in red. Right panel: Photo of snow patches in the Daisetsu mountains taken 28.06.2017 (Photo: K. Aalstad).

- Shuttle Radar Topography Mission (SRTM) DEM → resampled.
- ERA-Interim reanalysis temperature and precipitation → downscaled using the TopoSCALE approach.
- TOA reflectances from Landsat 8 and Sentinel-2 → NDSI snow mapping and aggregation.

Same ensemble DA framework but using a degree-day model.

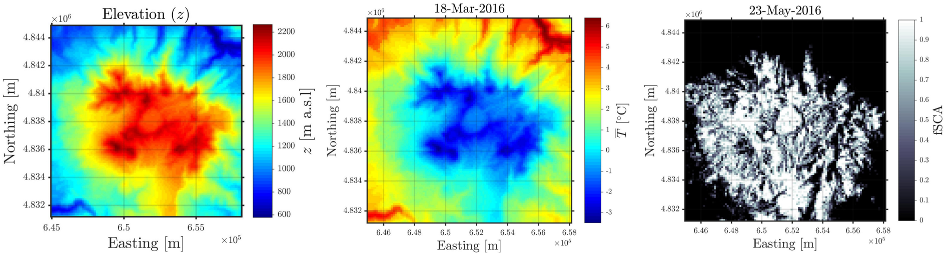

Figure : Left: SRTM resampled 120 m-DEM; Middle: Downscaled ERA-Interim temperature field, Right: fSCA retrieval from Sentinel-2A.

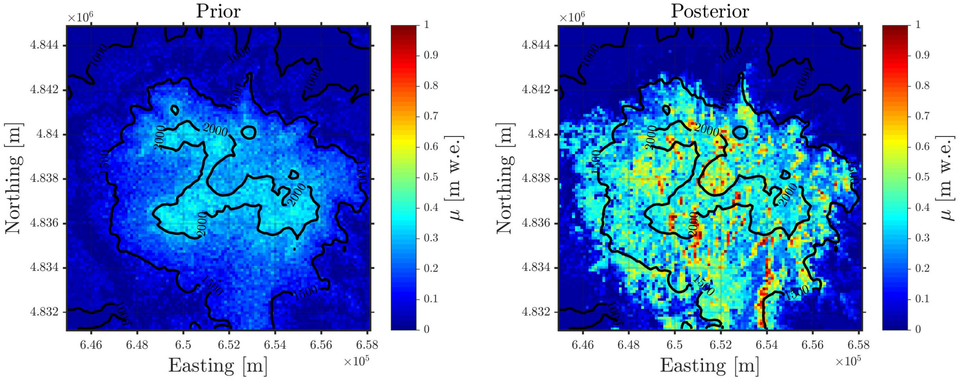

Figure : Daisetsu mountains, 2016 snow season. Left: Prior ensemble median peak mean SWE estimate, Right: Posterior Ensemble median peak mean SWE estimate.

Figure : Left panel: Location of the Izas catchment (Spanish Pyrenees) marked in red. Right panel: Time-lapse photo of the catchment during the melt season (Revuelto et al., 2017).

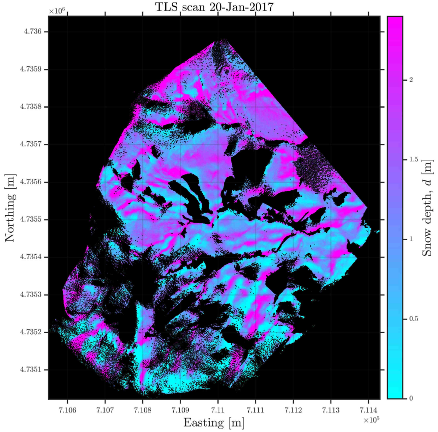
TLS scan 20-Jan-2017
Northing [m]
Easting [m]
Snow depth, d [m]
×10^6
×10^5
4.736
4.7359
4.7358
4.7357
4.7356
4.7355
4.7354
4.7353
4.7352
4.7351
7.106
7.107
7.108
7.109
7.11
7.111
7.112
7.113
7.114
0
0.5
1
1.5
2

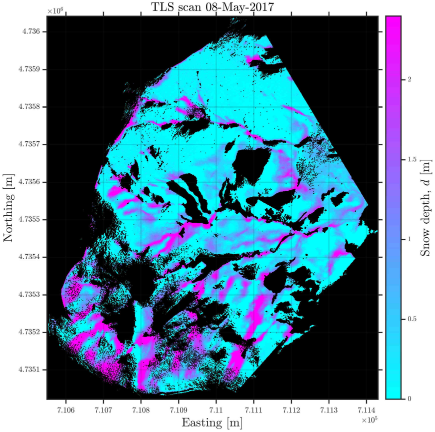
TLS scan 08-May-2017
Northing [m]
Easting [m]
Snow depth, d [m]
×10^6
×10^5
4.736
4.7359
4.7358
4.7357
4.7356
4.7355
4.7354
4.7353
4.7352
4.7351
7.106
7.107
7.108
7.109
7.11
7.111
7.112
7.113
7.114
0
0.5
1
1.5
2

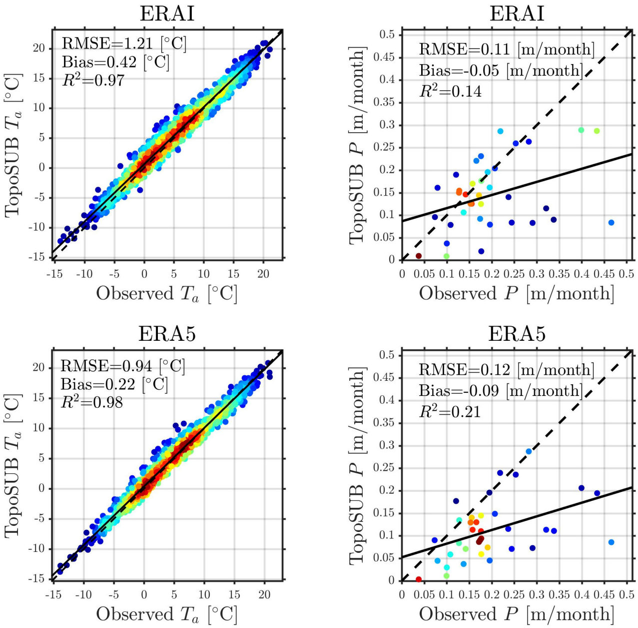
ERAI
RMSE=1.21 [°C]
Bias=0.42 [°C]
R^2=0.97
TopoSUB T_a [°C]
Observed T_a [°C]
ERAI
RMSE=0.11 [m/month]
Bias=-0.05 [m/month]
R^2=0.14
TopoSUB P [m/month]
Observed P [m/month]
ERA5
RMSE=0.94 [°C]
Bias=0.22 [°C]
R^2=0.98
TopoSUB T_a [°C]
Observed T_a [°C]
ERA5
RMSE=0.12 [m/month]
Bias=-0.09 [m/month]
R^2=0.21
TopoSUB P [m/month]
Observed P [m/month]

Landsat 8 (NASA&USGS): 2013-present, $\Delta t = 16$ days, $\Delta x = 30$ m, bands = B,G,R,NIR,SWIR

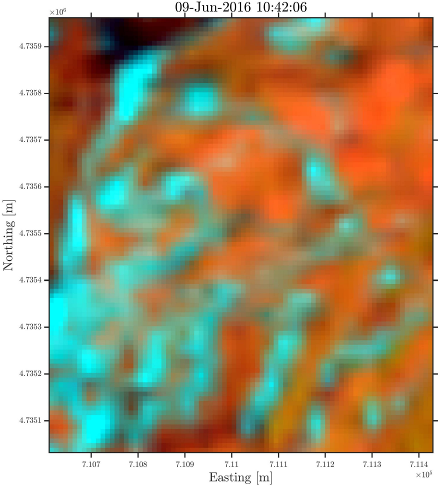

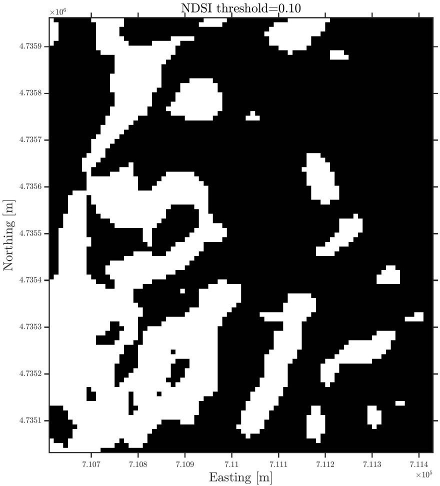

Sentinel-2A/2B (ESA): 2015/2017-present, $\Delta t = 5$ days, $\Delta x = 10$ m, Bands = B,G,R,NIR,SWIR.

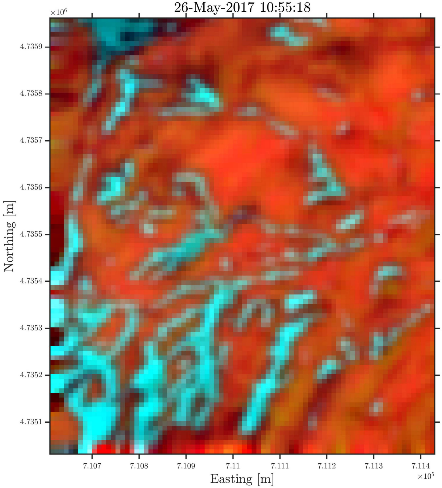

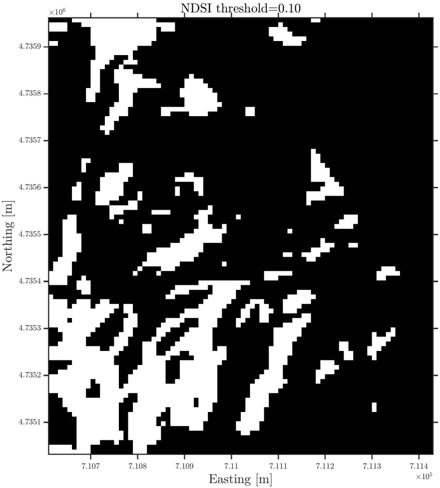

PlanetScope (planet.com) ~120 cubesats:

2014/2017-present,
$\Delta t = 1$ day,
$\Delta x = 3$ m,
Bands = B,G,R,NIR.

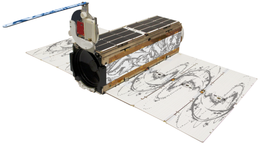

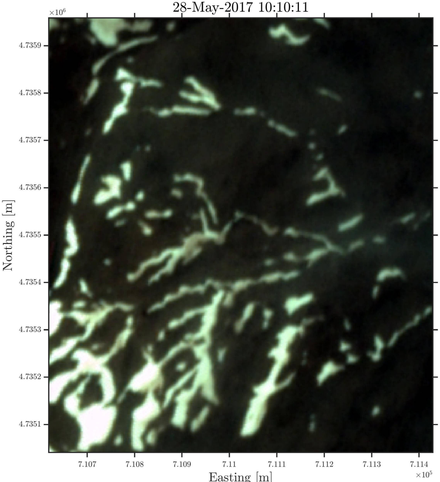

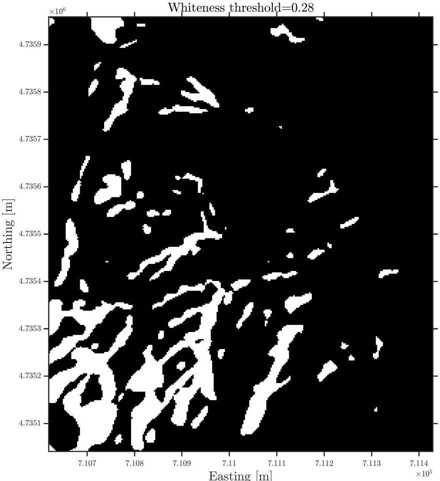

RapidEye (planet.com), 5 satellites: 2008-present, Δt = irregular (ca. 12 days), Δx = 5 m, Bands = B,G,R,NIR.

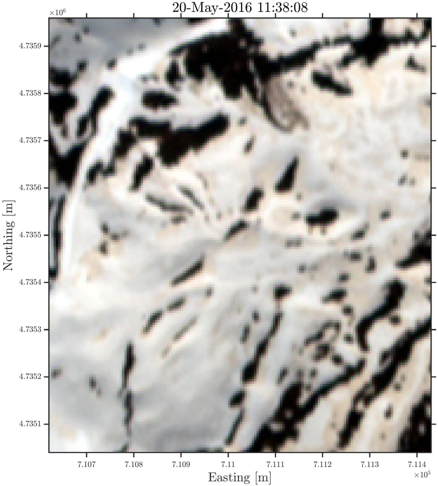

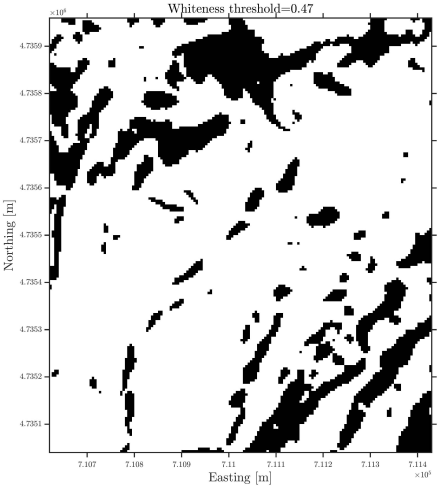

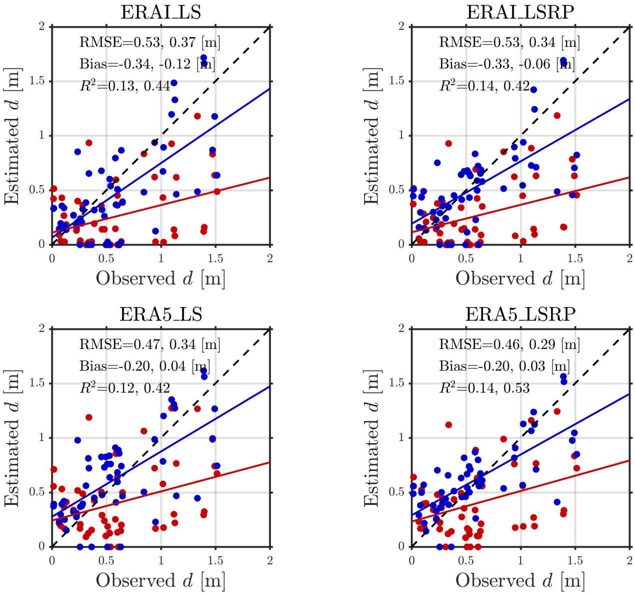
ERAI_LS
RMSE=0.53, 0.37 [m]
Bias=-0.34, -0.12 [m]
R^2=0.13, 0.44
ERAI_LSRP
RMSE=0.53, 0.34 [m]
Bias=-0.33, -0.06 [m]
R^2=0.14, 0.42
ERA5_LS
RMSE=0.47, 0.34 [m]
Bias=-0.20, 0.04 [m]
R^2=0.12, 0.42
ERA5_LSRP
RMSE=0.46, 0.29 [m]
Bias=-0.20, 0.03 [m]
R^2=0.14, 0.53
Estimated d [m]
Observed d [m]
0
0.5
1
1.5
2

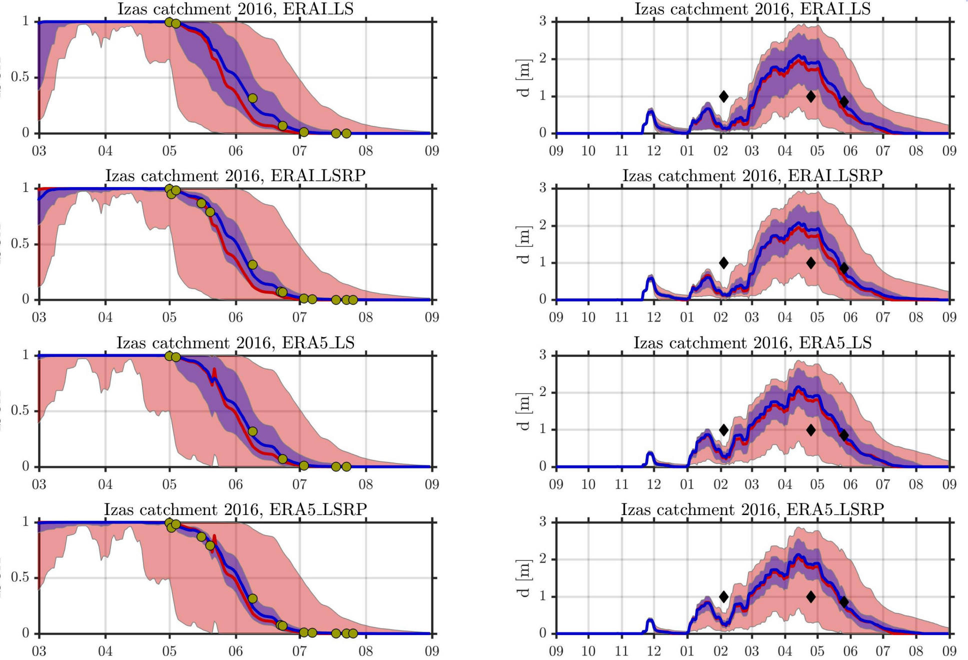
Izas catchment 2016, ERAI_LS
Izas catchment 2016, ERAI_LS
Izas catchment 2016, ERAI_LSRP
Izas catchment 2016, ERAI_LSRP
Izas catchment 2016, ERA5_LS
Izas catchment 2016, ERA5_LS
Izas catchment 2016, ERA5_LSRP
Izas catchment 2016, ERA5_LSRP
d [m]
03 04 05 06 07 08 09
09 10 11 12 01 02 03 04 05 06 07 08 09

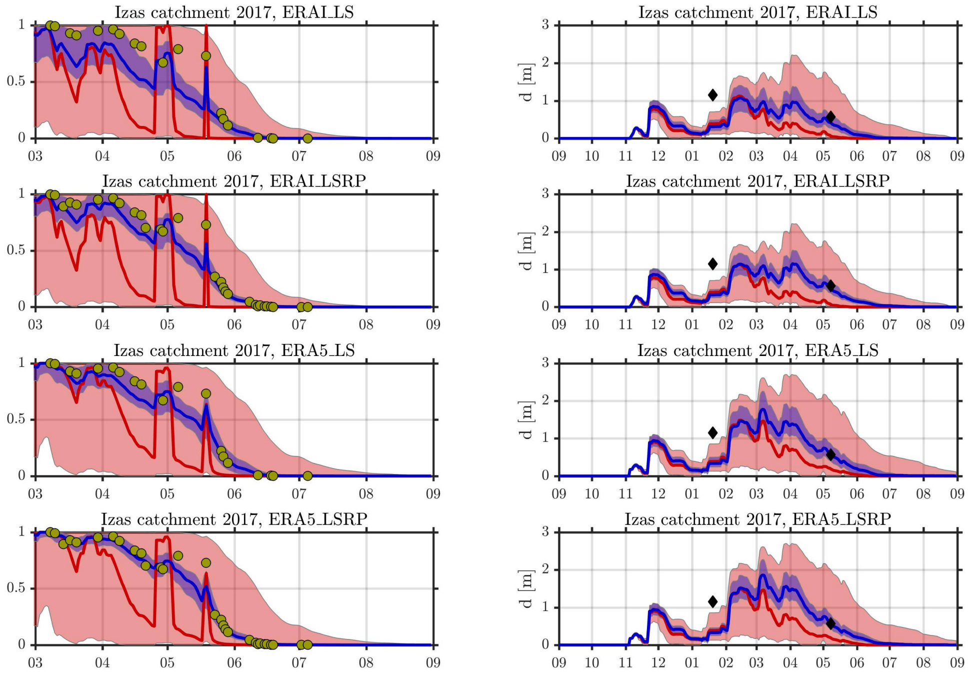
Izas catchment 2017, ERAI_LS
Izas catchment 2017, ERAI_LS
Izas catchment 2017, ERAI_LSRP
Izas catchment 2017, ERAI_LSRP
Izas catchment 2017, ERA5_LS
Izas catchment 2017, ERA5_LS
Izas catchment 2017, ERA5_LSRP
Izas catchment 2017, ERA5_LSRP
d [m]
0
0.5
1
2
3
03
04
05
06
07
08
09
10
11
12
01
02

- Reconstructing the seasonal snow at relatively high resolution (1 km - 100 m) while accounting for the inherent uncertainties in hydrometeorological forcing and satellite retrievals is feasible using an ensemble-DA framework.
- The main caveat to the success of this method is still the quality of the reanalysis precipitation field and the persistence of cloud cover during the melt season.
- The (relatively) accurate and representative Bayesian snow reconstruction estimates can be useful for evaluating land surface models and investigating the effect of snow parametrizations, particularly snow depletion curves, in remote regions where in-situ observations don't exist.
- Outlook: Evaluate Bayesian reconstruction results against ASO, continue investigating the relative importance of forcing and retrieval uncertainty, address model structural error using a Factorial Snow Model-like approach, couple the reconstruction to permafrost models.

Thank you, questions?

Durand, M., Molotoch, N. P., and Margulis, S. A. (2008). A Bayesian approach to snow water equivalent reconstruction. *Journal of Geophysical Research*, 113, D20117. doi: 10.1029/2008JD009894.

Emerick, A. A. and Reynolds, A. C. (2013). Ensemble smoother with multiple data assimilation. *Computers & Geosciences*, 55:3–15. doi: 10.1016/j.cageo.2012.03.011.

Fiddes, J. and Gruber, S. (2014). TopoSCALE v.1.0: downscaling gridded climate data in complex terrain. *Geoscientific Model Development*, 7:387–405. doi: 10.5194/gmd-7-387-2014.

Lahoz, W. A. and Schneider, P. (2014). Data Assimilation: Making Sense of Earth Observation. *Frontiers in Environmental Science*, 2(16). doi: 10.3389/fenvs.2014.00016.

Liston, G. E. (2004). Representing Subgrid Snow Cover Heterogeneities in Regional and Global Models. *Journal of Climate*, 17(6):1381–1397. doi: 10.1175/1520-0442(2004)017<1381:RSSCHI>2.0.CO;2.

Reichle, R. H. (2008). Data assimilation methods in the Earth sciences. *Advances in Water Resources*, pages 1411–1418. doi: 10.1016/j.advwatres.2008.01.001.

Revuelto, J. et al. (2017). Meteorological and snow distribution data in the Izas Experimental Catchment (Spanish Pyrenees) from 2011 to 2017. *ESSD*, 9:993–1005. doi: 10.5194/essd-9-993-2017.

Schuler, T., Crochet, P., Hock, R., Jackson, M., Barstad, I., and Johannesson, T. (2008). Distribution of snow accumulation on the Svartisen ice cap, Norway, assessed by a model of orographic precipitation. *Hydrological processes*, 22(19):3998–4008. doi: 10.1002/hyp.7073.

Slater, A. G., Barrett, A. P., Clark, M. P., Lundquist, J. D., and Raleigh, M. S. (2013). Uncertainty in seasonal snow reconstruction: Relative impacts of model forcing and image availability. *Advances in Water Resources*, 55:165–177. doi: 10.1016/j.advwatres.2012.07.006.

Westermann, S., Østby, T. I., Gisnås, K., Schuler, T. V., and Etzelmüller, B. (2015). A ground temperature map of the North Atlantic permafrost region based on remote sensing and reanalysis data. *The Cryosphere*, 9:1303–1319. doi: 10.5194/tc-9-1303-2015.